The Derivative free trust-region method for the inverse elastography problem

Sílvia Barbeiro[1], Rafael Henriques[1] and José Luis Santos[1]

University of Coimbra, Department of Mathematics, CMUC, 3000-143 Coimbra, Portugal
silvia@mat.uc.pt, rafael.henriques@mat.uc.pt, zeluis@mat.uc.pt

Abstract. In this work we investigate a mathematical model to reconstruct the mechanical properties of an elastic medium, for the optical coherence elastography imaging modality. To this end, we start by considering a mathematical model for the mechanical deformation based on time-harmonic equations of linear elasticity. The mathematical model for solving this direct problem is the computational basis to address the inverse problem which consists of determining the set of parameters that characterize the mechanical properties of the medium knowing the displacement field for a given excitation. We formulate the inverse problem as PDE-constrained optimization problem, where the objective function measures the discrepancy between observations and predictions. We propose a derivative free trust-region method to solve this inverse problem and we report several computational results which illustrate its behavior in terms of accuracy and efficiency.

Keywords: derivative free trust-region method, inverse problem, linear elasticity, mechanical properties reconstruction

1 Linear elasticity model

Let us consider an isotropic elastic material in the configuration space $\Omega \subseteq \mathbb{R}^3$, where Ω is a polyhedron with boundary $\partial\Omega$. The aim is to characterize the field of induced displacements, $\mathbf{u}(x,t)$ with $x \in \Omega$ and $t \in \mathbb{R}_0^+$.

Let us consider a sinusoidal excitation. The displacement has a time-harmonic form given by [7],

$$\mathbf{u}(x,t) = \Re\left(\mathbf{u}(x)\, e^{i\omega t}\right), \tag{1}$$

where $\Re$ is the real part of a complex and ω is the angular frequency of the sinusoidal excitation. For time-harmonic elastic propagation, the elastic displacement field $\mathbf{u}$ satisfies the Lamé equation

$$\mu\nabla^2\mathbf{u} + (\lambda+\mu)\nabla(\nabla\cdot\mathbf{u}) + \omega^2\rho\mathbf{u} + \mathbf{f} = 0 \text{ in } \Omega \tag{2}$$

where ρ is the material density, $\mathbf{f}$ is a given distribution of body forces and the Lamé constants μ and λ are given, respectively, by

$$\mu = \frac{E}{2(1+\nu)} \text{ and } \lambda = \frac{\nu E}{(1+\nu)(1-2\nu)},$$

being E is the Young's Modulus and ν is the Poisson's ratio.

Let Γ_1 and Γ_2 be two open subsets of $\partial\Omega$ such that $\partial\Omega = \overline{\Gamma}_1 \cup \overline{\Gamma}_2$, $\Gamma_1 \cap \Gamma_2 = \emptyset$ and $\text{meas}(\Gamma_2) > 0$. We impose the traction boundary condition on Γ_1

$$\sigma(\mathbf{u})\eta = \mathbf{g} \text{ on } \Gamma_1, \tag{3}$$

where η is the unit outer normal direction. The stress tensor is given by

$$\sigma(\mathbf{u}) = 2\mu\varepsilon(\mathbf{u}) + \lambda \text{tr}(\varepsilon(\mathbf{u}))\text{I}$$

where ε is the strain tensor

$$\varepsilon(\mathbf{u}) = \frac{1}{2}\left(\nabla\mathbf{u} + (\nabla\mathbf{u})^\intercal\right).$$

Here I is the 3×3 identity matrix and $\text{tr}(\varepsilon(\mathbf{u}))$ is the trace of $\varepsilon(\mathbf{u})$. It is assumed that the medium is fixed on some non-empty open set Γ_2, where we impose displacement boundary condition

$$\mathbf{u} = 0 \text{ on } \Gamma_2. \tag{4}$$

To solve this direct problem, we consider the classic finite element method (FEM) which consists of using degree one piecewise polynomials in the approximation. For the case of a nearly incompressible materials, *i.e.* with Poisson's ratio ν close to 0.5, the performance of a classical FEM scheme can deteriorate due to the locking as $\nu \to 0.5$ [1]. Here we are assuming that we are dealing with media for which the range of values of the Poisson's ratio leads to locking-free FEM solutions. As an example of application, we can mention the aortic elastography [2]. For general materials, some numerical methods have been proposed in the literature, in particular some variations of mixed finite element methods.

To derive the finite element method, we need to consider the weak form of the mathematical model. Let $V = \left\{\mathbf{v} \in H^1(\Omega) : \mathbf{v}|_{\Gamma_2} = 0\right\}$. The weak formulation of (2)–(4) reads: find $\mathbf{u} \in V$ such that

$$a(\mathbf{u}, \mathbf{v}) = l(\mathbf{v}), \ \forall \mathbf{v} \in V, \tag{5}$$

where

$$a(\mathbf{u}, \mathbf{v}) = \int_\Omega 2\mu\varepsilon(\mathbf{u}) : \varepsilon(\mathbf{v}) + \lambda(\nabla \cdot \mathbf{u})(\nabla \cdot \mathbf{v}) - \omega^2\rho\mathbf{u} \cdot \mathbf{v}\, dx \tag{6}$$

and

$$l(\mathbf{v}) = \int_{\Gamma_1} \mathbf{g} \cdot \mathbf{v}\, ds + \int_\Omega \mathbf{f} \cdot \mathbf{v}\, dx.$$

Let us consider a partition of Ω into M tetrahedra K_j, $j \in \{1, ..., M\}$ so that

$$\Omega = \bigcup_{j=1}^{M} K_j \text{ and } \text{int}(K_i) \cap \text{int}(K_j) = \emptyset, \forall\, i, j \in \{1, ..., M\}, \ i \neq j. \tag{7}$$

The resulting subdivision (or mesh) is denoted by Ω_h where h represents the diameter of the partition. To each tetrahedron there are associated four vertices

that can be either in the interior or on the border of Ω. For any pair of open tetrahedra in the partition K_i and K_j, $i \neq j$, $\overline{K}_i \cap \overline{K}_j$ is either empty, or a common vertex, side or face of K_i and K_j.

Let us consider the finite dimensional subspace $V_h \subset V$ of continuous functions which are linear on each tetrahedron. Assuming that N is the total number of vertices in Ω_h then $\dim V_h = 3N$. The finite element formulation of the problem (5) can be written as: find $\mathbf{u}_h \in V_h$ such that

$$a(\mathbf{u}_h, \mathbf{v}_h) = l(\mathbf{v}_h), \ \forall \mathbf{v}_h \in V_h. \tag{8}$$

Let $V_h = \text{span}\left\{\phi_{11}, ..., \phi_{N1}, \phi_{12}, ..., \phi_{N2}, \phi_{13}, ..., \phi_{N3}\right\}$, where ϕ_{ji}, $i = \{1, 2, 3\}$, $j = \{1, ..., N\}$, are the linearly independent basis functions, $\phi_{ji}(x^j) = 1$, $\phi_{ji}(x^k) = 0$ $(k \neq j)$, and the support of ϕ_{ji} consists in all tetrahedra that share x^j as a vertex. In this way, each component of the approximate solution $\mathbf{u}_h = (u_{1h}, u_{2h}, u_{3h}) \in V_h$ can be written as a linear combination of the basis functions ϕ_{ji} with

$$u_{ih}(x) = \sum_{j=1}^{N} U_{ji}\phi_{ji}\left(x\right), \ i = 1, 2, 3, \tag{9}$$

where U_{ji}, $i = \{1, 2, 3\}$, $j = \{1, ..., N\}$ are the coefficients that we want to calculate. Problem (8) is then equivalent to a linear system in the form

$$AU = F, \tag{10}$$

where $U = [U_{11}, ..., U_{N1}, U_{12}, ..., U_{N2}, U_{13}, ..., U_{N3}]^\intercal$, A is a $3N \times 3N$ matrix which depends on the parameters μ and λ, and F a vector of dimension $3N$. A is a non-singular matrix so (10) has a unique solution.

2 Inverse problem

In this section we will analyze the inverse problem, which can be described by the following minimization program:

$$\begin{array}{ll} \min\limits_{\mu,\ \lambda} & \|U - U_{obs}\|^2_{L^2_h(\Omega)} \\ \text{s.t.} & AU = F \\ & \mu \in [\mu_1, \mu_2] \\ & \lambda \in [\lambda_1, \lambda_2] \end{array},$$

which can be rewritten as

$$\begin{array}{ll} \min\limits_{\mu,\ \lambda} & \left\|A^{-1}F - U_{obs}\right\|^2_{L^2_h(\Omega)} \\ \text{s.t.} & \mu \in [\mu_1, \mu_2] \\ & \lambda \in [\lambda_1, \lambda_2] \end{array}, \tag{11}$$

where A and F define the linear system to solve the direct problem (10) and U_{obs} is the vector that contains the information of the given data on the vertices

of the mesh. Here we use the discrete L^2_h-norm, defined for any $3N \times 1$ vector y, as

$$\|y\|^2_{L^2_h(\Omega)} = \sum_{K \in \Omega_h} \|y\|^2_{L^2_h(K)},$$

with

$$\|y\|^2_{L^2_h(K)} = \frac{|K|}{4} \sum_{i=1}^{4} \sum_{j=0}^{2} y^2_{t(r_i)+jN},$$

where $|K|$ denotes the volume of the tetrahedron K with vertices $r_i, i \in \{1, \ldots, 4\}$. The function t is defined by

$$\begin{array}{rl} t : \mathbb{R}^3 & \to \{1, ..., N\} \\ r_i & \mapsto \quad t(r_i), \end{array}$$

where $t(r_i)$ is the index that corresponds to vertex of r_i in the global numbering.

We are assuming that the range of values for μ and λ set in (11) are compatible with the biological structures.

For convenience, in what follows, we denote the objective function by $l(\mu, \lambda)$, that is,

$$l(\mu, \lambda) = \left\| A^{-1}F - U_{obs} \right\|^2_{L^2_h(\Omega)}. \tag{12}$$

3 Derivative free trust-region method

The configuration of the function l seems to be well approximate, locally, by a quadratic function. This fact, motivated us to apply a variation version of the trust region method presented in [15] where a quadratic model is used to approximate the objective function.

Usually trust region method is based on Taylor's series expansion of l around (μ_k, λ_k) [10]. To avoid the computation of the derivatives of l, we consider the least squares method to get the quadratic model which approximates $l(\mu, \lambda)$ using a set

$$P_k = \{(\mu_{i,k}, \lambda_{i,k}) : i \in \{1, ..., n_k\}\}$$

with $n_k \geq 9$ random points where the function l is known. Let us consider that these n_k points belong to the set $I_k = [\mu_{inf,k}, \mu_{sup,k}] \times [\lambda_{inf,k}, \lambda_{sup,k}]$ and that, each of the nine sub-sets, which correspond to each of the cells in a uniform 3×3 grid in the set I_k:

$$I_{i,j,k} = [\mu_{inf,k} + (i-1)s_k, \mu_{inf,k} + is_k] \times [\lambda_{inf,k} + (j-1)r_k, \lambda_{inf,k} + jr_k], \tag{13}$$

$i, j = 1, 2, 3$, where $s_k = \frac{1}{3}(\mu_{sup,k} - \mu_{inf,k})$, $r_k = \frac{1}{3}(\lambda_{sup,k} - \lambda_{inf,k})$. We impose that each sub-sets contains at least one point to make sure that the points are not too close to each other and to have representative points around all the trust region. Moreover, we assume that (μ_k, λ_k) belongs to the central sub-set, that is, $(\mu_k, \lambda_k) \in I_{2,2,k}$.

With these n_k points, we want to derive the k-th quadratic model l_k, that can be written in the form

$$l_k(\mu,\lambda) = a_1 + a_2\mu + a_3\lambda + a_4\mu^2 + a_5\lambda^2 + a_6\mu\lambda,\ k \in \mathbb{Z}_0^+, \tag{14}$$

for some $a_i \in \mathbb{R}$, $i \in \{1,...,6\}$. The coefficients a_i, $i \in \{1,...,6\}$, are determined in way to minimize the function

$$L_k(a_1,...,a_6) = \sum_{i=1}^{n_k} \left(l(\mu_{i,k},\lambda_{i,k}) - l_k(\mu_{i,k},\lambda_{i,k})\right)^2.$$

The necessary condition to obtain the solution is

$$\frac{\partial L_k}{\partial a_i}(a_1,...,a_6) = 0, i \in \{1,...,6\} \tag{15}$$

and the solution $a^* = (a_1^*,\ldots,a_6^*)$ of this system exists and it is unique [6].

It now remains to characterize the minimizer of l_k through the trust region. Let (μ_0,λ_0) be the initial point and $\Delta_0 > 0$ the initial trust region radius. So the initial trust-region is defined by the set I_0 such that $(\mu_0,\lambda_0) \in I_{2,2,0}$ and for the other sub-sets a random point is generated. After defining the set P_0 with these points, we are able to calculate l_0. For the iteration k let us consider the points of P_k to obtain the k-th approximation l_k by the least squares method. To achieve the minimizer, we will obtain the solution of the next sub-problem

$$\begin{array}{ll} \min\limits_{(\mu,\lambda)\in\mathbb{R}^2} & l_k(\mu,\lambda) \\ \text{s.t.} & \|(\mu,\lambda) - (\mu_k,\lambda_k)\|_\infty \leq \Delta_k. \end{array} \tag{16}$$

The solution $(\mu_{k+1},\lambda_{k+1})$ will be the minimizer of l_k in the square centered in (μ_k,λ_k) and radius Δ_k. The critical point is the solution of $\nabla l_k(\mu,\lambda) = 0$, that is,

$$\begin{bmatrix} 2a_4^* & a_6^* \\ a_6^* & 2a_5^* \end{bmatrix} \begin{bmatrix} \mu \\ \lambda \end{bmatrix} = - \begin{bmatrix} a_2^* \\ a_3^* \end{bmatrix} \tag{17}$$

where a_i^*, $i \in \{2,\cdots,6\}$ are the solution of (15). We note that the matrix of the system (17) is the hessian, $\nabla^2 l_k(\mu,\lambda)$, of the quadratic model (14). The correspondent eigenvalues are given by

$$a_4^* + a_5^* \pm \sqrt{(a_4^* - a_5^*)^2 + (a_6^*)^2}.$$

So this values are both positive when $4a_4^*a_5^* - (a_6^*)^2 > 0$ and $a_4^* > 0$.

If the hessian is positive definite and the solution obtained by resolution of (17) is in the trust region, the solution of (17) is the minimizer of (16). If one of this conditions is not satisfied the minimizer will be determined on the boundary.

Let (μ_k^*,λ_k^*) denote the minimizer of (16) in the iteration k. To accept this minimizer, we analyze the ratio

$$\rho_k = \frac{l(\mu_k,\lambda_k) - l(\mu_k^*,\lambda_k^*)}{l_k(\mu_k,\lambda_k) - l_k(\mu_k^*,\lambda_k^*)} \tag{18}$$

and we compare it with the value $\gamma \in]0,1[$ initially fixed, where γ is a parameter of the trust-region method that defines whether the iteration is successful. If $\rho_k \geq \gamma$, the objective function is well fitted by the quadratic model and we accept the (μ_k^*, λ_k^*) as the new approximation $((\mu_{k+1}, \lambda_{k+1}) = (\mu_k^*, \lambda_k^*))$, $\Delta_{k+1} = \Delta_k$; otherwise, the trust region is too large and the fit between the function and the model is not satisfatory. In this case, we keep the previous approximation $((\mu_{k+1}, \lambda_{k+1}) = (\mu_k, \lambda_k))$ and reduce the trust region radius $(\Delta_{k+1} = \Delta_k/2)$.

To update P_{k+1} and I_{k+1}, regardless of whether the iteration is successful or not, the new trust region I_{k+1} is the square centered on $(\mu_{k+1}, \lambda_{k+1})$ with radius Δ_{k+1} so $(\mu_{k+1}, \lambda_{k+1}) \in I_{2,2,k+1}$. Additionally, we keep the points $P_k \cap I_{k+1}$ in the corresponding sub-set. Finally, we generate a random point on each sub-set $I_{i,j,k+1}$ that remains empty. P_{k+1} is the set with the new n_{k+1} points obtained by this process and a new quadratic model is obtained by the least squares method. We would like to emphasize that only the admissible portion of each sub-set is considered in I_k.

This procedure is repeated until the relative error between two consecutive iterations is less than 10^{-5} on both parameters. Algorithm 1 presents the sketch of this procedure which is a variation of the derivative free trust-region method presented in [15].

Algorithm 1: Derivative free trust-region method

Initialization Choose (μ_0, λ_0) such that $l(\mu_0, \lambda_0) < \infty$, $\Delta_0 > 0$ and the constant $\gamma \in]0,1[$. Obtain I_0 and consequently P_0. Define $k = 0$.
repeat
  Construct the model for $l_k(\mu, \lambda)$ by the least squares method applied to (15) with the points of P_k.
  Obtain the critical point by solving problem (17).
  if $\nabla^2 l_k(\mu, \lambda)$ is positive definite and satisfies the constrain of the sub-problem (16) **then**
    (μ_k^*, λ_k^*) is the minimizer;
  else
    Obtain the minimizer (μ_k^*, λ_k^*) over the boundary of the square centered in (μ_k, λ_k) and radius Δ_k.
  Calculate ρ_k in (18).
  if $\rho_k \geq \gamma$ **then**
    $\Delta_{k+1} = \Delta_k$;
    $(\mu_{k+1}, \lambda_{k+1}) = (\mu_k^*, \lambda_k^*)$;
  else
    $\Delta_{k+1} = \Delta_k/2$;
    $(\mu_{k+1}, \lambda_{k+1}) = (\mu_k, \lambda_k)$;
  Update I_{k+1}, P_{k+1} as described in this section.
  $k = k + 1$;
until $\frac{|\mu_k - \mu_{k-1}|}{\mu_{k-1}} < 10^{-5} \wedge \frac{|\lambda_k - \lambda_{k-1}|}{\lambda_{k-1}} < 10^{-5}$;

4 Computational results

Let us consider the objective function defined by (12), which corresponds to the following setting: $\Omega = [-2,2]^3$ with $\partial\Omega = \Gamma_1 \cup \Gamma_2$ where Γ_1 is the face of the cube contained in the plane $z = -2$; the mesh is a partition of Ω into 48 tetrahedrons; $\rho = 1$, $w = 2\pi \times 10^6$; the functions $\mathbf{g}$ and $\mathbf{f}$ are defined respectively by $g_i = 5.86 \times 10^{-3}$ and $f_i = 0$, $i \in \{1,2,3\}$.

To illustrate the performance of the proposed method we used fabricated data obtained by simulating the direct problem. In particular, we considered U_{obs} as the solution of (10) with $E = 4.66 \times 10^6$ and $\nu = 0.45$ [2]. In this way, $(\mu, \lambda) = (1.6069 \times 10^6, 1.4462 \times 10^7)$ is the optimal solution of the inverse problem. For the optimization problem we choose the set $I = [0.9\mu, 1.1\mu] \times [0.9\lambda, 1.1\lambda]$ and we define $\Delta_0 = 10^5$ ($\Delta_0 < 0.1 \max\{\mu, \lambda\}$) and $\gamma = 0.1$.

In the context of a real application, experimental data are affected by noise. Here we performed experiments with noise free data as well as noisy data in order to assess the sensitivity of our method to noise.

To check the robustness of the proposed method when considering noisy data we consider gaussian noise $R \sim N(0, \sigma)$ where R is a random vector of dimension $3N \times 1$ and σ is the standard deviation. So instead U_{obs}, we consider as data $\bar{U}_{obs} = (R + 1_{3N\times 1})U_{obs}$, where $1_{3N\times 1}$ is a $3N \times 1$ vector with all components equal to one and the i-th component of the vector $\bar{U}_{obs}$ is given by $(R(i) + 1)U_{obs}(i)$, $i \in \{1, ..., 3N\}$.

We consider variations of σ in the set $\left\{0, 10^{-8}, 10^{-7}, 10^{-6}, 10^{-5}\right\}$ and, for each value of σ, we consider simulations with 30 random initial points.

Figure 1 presents the relative error averages $\dfrac{|\mu_k - \mu_{k-1}|}{\mu_{k-1}}$ and $\dfrac{|\lambda_k - \lambda_{k-1}|}{\lambda_{k-1}}$ obtained from thirty simulations for each value of σ. As expected, increasing the number of iterations has the effect of decreasing the relative error between two consecutive iterations, allowing the approximations to converge close to the optimal solution and satisfy the stop condition. As we can be seen in Figure 1, the performance of Algorithm 1 is not significantly affected by the increase in noise.

Now since we have the thirty approximations for each value of σ, we will show in Figure 2 the evolution of the relative error average between the approximation given by the method and the solution $(\mu, \lambda) = (1.6069 \times 10^6, 1.4462 \times 10^7)$. As expected, both parameters show an increase in the average error with σ, which can lead to large perturbations in the optimal solution. Although the noise variation is not high, it generates higher relative errors comparing to the case of no noise ($\sigma = 0$). In Figure 2 we can see that for $\sigma \in \left\{10^{-6}, 10^{-5}\right\}$ the relative error in μ is very closed to 0.1. This situation happens because the level of noise considered change the behaviour of the objective function where the minimum in attained in the boundary of I. Note that in the boundary of the domain I the approximations achieve relative error of the order 0.1.

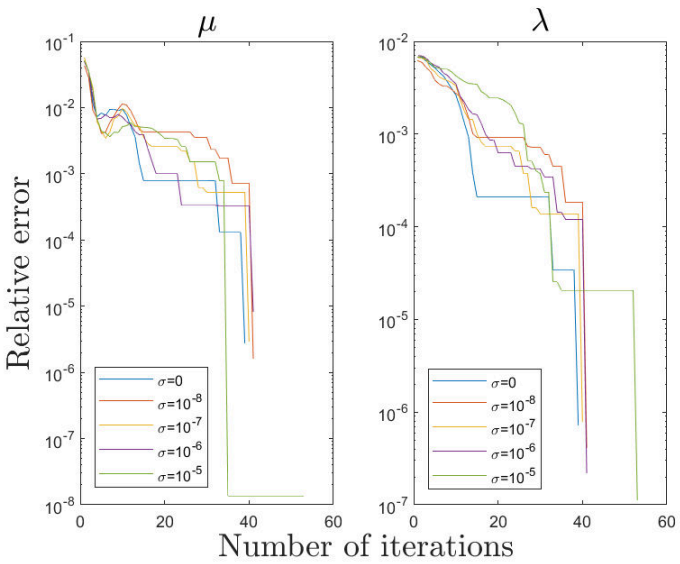

Fig. 1: Relative error average obtained from thirty simulations for the parameters μ (left) and λ (right) considering different levels of noise.

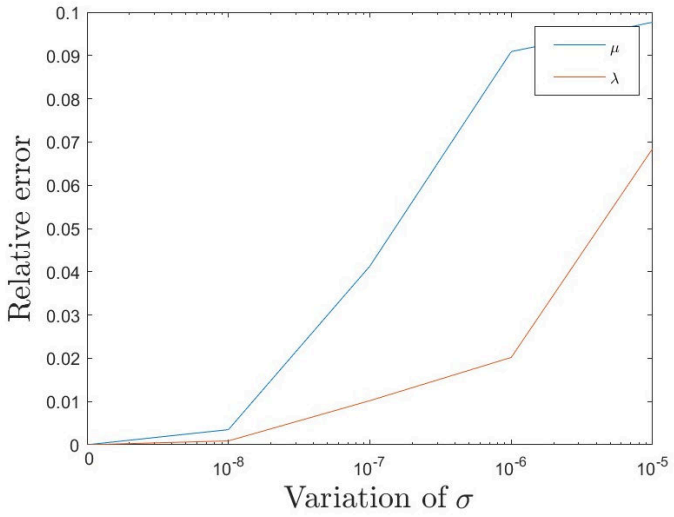

Fig. 2: Relative error average obtained from thirty simulations for each value of σ.

References

1. M. Ainsworth, C. Parker. Unlocking the secrets of locking: Finite element analysis in planar linear elasticity. Computer Methods in Applied Mechanics and Engineering, 395, 2022.
2. G. Giannakoulas , G. Giannoglou, J. Soulis, T. Farmakis, S. Papadopoulou, G. Parcharidis, G. Louridas. A computational model to predict aortic wall stresses in patients with systolic arterial hypertension. Elsevier, Medical Hypotheses, 2005.
3. S. Barbeiro, P. Serranho. The method of fundamental solutions for the direct elastography problem in the human retina. Proceedings of the 9th Conference on Trefftz Methods and 5th Conference on Method of Fundamental Solutions, Springer, 2020.
4. Susane C. Brenner, L. Ridgway Scott. The Mathematical Theory of Finite Element Methods. Springer, 1997.
5. D. Claus, M. Mlikota, J. Geibel, T. Reichenbach, G. Pedrini, J. Mischinger, S. Schmauder, and W. Osten. Large-field-of-view optical elastography using digital image correlation for biological soft tissue investigation. Journal of Medical Imaging, 4 (1): 1–14, 2017.
6. Andrew R. Conn, Katya Scheinberg, and Luís N.Vicente. Geometry of sample sets in derivative free optimization: polynomial regression and undertermined interpolation, 2008.
7. M. M. Doyley. Model-based elastography: a survey of approaches to the inverse elasticity problem. Physics in Medicine and Biology, 57 (3):R35-R73, 2012.
8. W. Hackbusch. Elliptic Differential Equations. Theory and Numerical Treatment, 1992.
9. B. F. Kennedy, X. Liang, S. G. Adie, D. K. Gerstmann, B. C. Quirk, S. A. Boppart, and D. D. Sampson. In vivo three-dimensional optical coherence elastography. Opt. Express, 19 (7):6623–6634, 2011.
10. J. Nocedal and S. J. Wright. Numerical Optimization. Berlin, Springer, 2006.
11. E. Park, A.M. Maniatty. Shear modulus reconstruction in dynamic elastography: time Harmonic case. Phys. Med. Biol. 51(15), 3697-3721, 2006.
12. Y. Qu, Y. He, Y. Zhang, T. Ma, J. Zhu, Y. Miao, C. Dai, M. Humayun, Q. Zhou, and Z. Chen. Quantified elasticity mapping of retinal layers using synchronized acoustic radiation force optical coherence elastography. Biomed.Opt.Express, 9 (9):4054–4063, 2018.
13. P. Serranho, S. Barbeiro, R. Henriques, A. Batista, M. Santos, C. Correia, J. Domingues, C. Loureiro, J. Cardoso, R. Bernardes, M. Morgado. On the Numerical Solution of the Inverse Elastography Problem for Time-harmonic Excitation. In Proceedings of the 2nd International Conference on Image Processing and Vision Engineering (IMPROVE 2022), pages 259-264, 2022.
14. J. Zhu, Y. Miao, L. Qi, Y. Qu, Y. He, Q. Yang, and Z. Chen. Longitudinal shear wave imaging for elasticity mapping using optical coherence elastography. Applied Physics Letters, 110 (20):201101, 2017.
15. Diogo Júdice. Trust-Region Methods without using Derivatives: Worst-Case Complexity and the Non-Smooth Case. University of Coimbra, 2015.

Acknowledgements

This work was partially supported by the Centre for Mathematics of the University of Coimbra (funded by the Portuguese Government through FCT/MCTES,

DOI 10.54499/UIDB/00324/2020); the FEDER Funds through the Operational Program for Competitiveness Factors - COMPETE and by Portuguese National Funds through FCT - Foundation for Science and Technology “2021.06672.BD”; the FCT (Portugal) research project PTDC/EMD-EMD/32162/2017, COMPETE and Portugal 2020.